Journal of Catalysis **196,** 104–114 (2000)
doi:10.1006/jcat.2000.3032, available online at http://www.idealibrary.com on IDEAL®

Promoting Effect of Al on SO_4^{2-}/M_xO_y (M = Zr, Ti, Fe) Catalysts

Weiming Hua, Yongde Xia, Yinghong Yue, and Zi Gao[1]

Department of Chemistry, Fudan University, Shanghai 200433, P.R. China

Received April 7, 2000; revised August 11, 2000; accepted August 22, 2000

The promoting effect of Al on various types of sulfated metal oxide catalysts has been studied. Incorporation of an appropriate amount of Al_2O_3 into zirconia, titania, and iron oxide before sulfation increases the acidity, activity, and stability of the catalysts for isomerization of *n*-butane and *n*-pentane significantly. The steady-state conversion of *n*-butane at 250°C and *n*-pentane at 300°C over 3 mol% Al_2O_3-promoted sulfated zirconia (SZA-3) are 2.2 and 4.5 times higher than those over unpromoted sulfate zirconia (SZ), respectively. In benzoylation of toluene with benzoyl chloride, after running for 10 h at 110°C the yield of methylbenzophenones on SZA-3 and SZ catalysts are 91.2 and 70.9%, respectively. The addition of Al_2O_3 helps to stabilize the surface sulfate complex on the oxides and increases the number of catalytically effective acid sites on the catalysts. Different from the promoting mechanism of Fe and Mn incorporated sulfated zirconia catalyst, the high catalytic activity and slow deactivation of the Al-promoted catalysts for *n*-alkane isomerization are caused by an increase in the number of intermediate–strong acid sites with differential heat of adsorption of NH_3 between 125 and 140 kJ mol^{-1}, providing long-term activity to the reaction.

Key Words: **Al-promoted sulfated oxides catalysts; *n*-butane isomerization; *n*-pentane isomerization; toluene benzoylation; acid strength distribution.**

INTRODUCTION

Acid catalysis plays a key role in many important reactions of the chemical and petroleum industries. Conventional industrial acid catalysts, such as sulfuric acid, $AlCl_3$, and BF_3, have unavoidable drawbacks because of their severe corrosivity and high susceptibility to water. The search for environmentally benign heterogeneous catalysts has driven the worldwide ongoing research of new materials as substitutes for current liquid acids and halogen-based solid acids (1). Among them sulfated oxides, such as sulfated zirconia, titania, and iron oxide, displaying high thermostability, very strong acidity, and high catalytic activity, have aroused increasing interest (2–6). At the beginning of this decade, Hsu *et al.* (7) have reported that doping sulfated zirconia with 1.5 wt% Fe and 0.5 wt% Mn increases the rate of *n*-butane isomerization on the catalyst by two to three orders of magnitude. The promotion in activity of this type of catalyst has been confirmed by several other research groups (8–10). Coelho *et al.* (11) have discovered that the addition of Ni to sulfated zirconia causes an activity enhancement comparable to that caused by the addition of Fe and Mn. Miao *et al.* (12, 13) have found that sulfated oxides of Cr–Zr, Fe–Cr–Zr, and Fe–V–Zr are two to three times more active than sulfated Fe–Mn–Zr for *n*-butane isomerization. The promoting effect of the transition metals in these catalysts is generally recognized to be related to a bifunctional mechanism of the isomerization reaction in which the presence of the transition metals accelerates the dehydrogenation of the reactant (14). However, these catalysts deactivate rapidly during isomerization of *n*-alkanes, e.g., the Fe and Mn promoted catalyst deactivates quickly at 60°C in the presence of N_2 and 250°C in the presence of H_2 (9, 15). In our previous work (16), it has been found that a main group element Al can also promote the catalytic activity and stability of SO_4^{2-}/ZrO_2 for *n*-butane isomerization. After being on stream for 120 h at 250°C, the *n*-butane conversion of an Al-promoted catalyst keeps steadily at 88% of its equilibrium conversion without observable deactivation.

Friedal Crafts acylation of aromatics is also an important strong acid-catalyzed reaction. New clean solid acid catalysts, such as Nafion-H (17), $FeSO_4$ (18), SO_4^{2-}/γ-Al_2O_3 (19), and SO_4^{2-}/ZrO_2 (19, 20) have been suggested to replace the conventional acid catalysts such as dehydrated $AlCl_3$. The Al-promoted catalyst prepared in our laboratory is also highly active for the benzoylation of toluene, with benzoyl chloride giving 100% yield of methylbenzophenones after being on stream for 12 h at 110°C (21).

In the present work, the promoting effect of Al on sulfated zirconia, titania, and iron oxide was studies systematically. The activity of the Al-promoted catalysts for *n*-alkane isomerization and benzoylation of toluene with benzoyl chloride with relation to Al content was investigated. The number and acid strength distribution of surface acid sites of the three series of catalysts containing different amount of Al_2O_3 were measured quantitatively by means of a microcalorimetric method. The activities of the Al-promoted

[1] To whom correspondence should be addressed. Fax: 86-21-65641740. E-mail: zigao@fudan.edu.cn.

0021-9517/00 $35.00

catalysts were correlated with the data of microcalorimetry and other characterization methods, such as XRD, TG-DTG, IR, MAS NMR, and XPS, and the nature of the promoting effect of Al was discussed.

EXPERIMENTAL

Sample Preparation

Aqueous ammonia was added dropwise to a solution of $ZrOCl_2$, $TiCl_4$, $Fe(NO_3)_3$, or $Al(NO_3)_3$ till pH 9–10. After washing, filtering, and drying at 110°C, the hydroxides of $Zr(OH)_4$, $Ti(OH)_4$, and $Al(OH)_3$ were then immersed in a 0.5 mol L^{-1} H_2SO_4 solution and the hydroxide of $Fe(OH)_3$ was immersed in a 0.25 mol L^{-1} H_2SO_4 solution for 30 min. The sulfated zirconia (SZ), sulfated alumina (SA), sulfated titania (ST), and sulfated iron oxide (SF) were dried at 110°C and then calcined at 650 or 500°C for 3 h. Al-promoted catalysts were prepared in the same way from a mixed solution of $ZrOCl_2$, $TiCl_4$, or $Fe(NO_3)_3$ and $Al(NO_3)_3$, and they were labeled as SZA, STA, and SFA respectively. For comparison, sulfated γ-Al_2O_3 was prepared by the method in the literature (19). γ-Al_2O_3 was immersed in a 2.5 mol L^{-1} H_2SO_4 solution for 30 min, filtered, dried at 110°C, and then calcined at 650°C for 3 h. The catalyst was labeled as SγA. SO_4^{2-}/1.5%Fe/0.5%Mn/ZrO_2 (SZFM) was prepared according to the procedures in the literature (12).

Characterization

X-ray powder diffraction measurements were performed on a Rigaku D/MAX-IIA instrument with Cu$K\alpha$ radiation at 40 kV and 20 mA, a scan speed of 16° min^{-1}, and a scan range of 5–70°. TG-DTG analysis was carried out on a Rigaku Thermoflex instrument in flowing air at a heating rate of 10 K min^{-1}. Infrared spectra of the samples were recorded on a Perkin-Elmer 983 G spectrometer. The samples were pressed into thin disks with a density of 3–5 mg cm^{-2} and placed in a quartz cell with CaF_2 windows. BET surface area of the samples was measured on a Micromeritics ASAP 2000 apparatus using N_2 as the adsorbent. ^{27}Al MAS NMR spectra were recorded at room temperature using a Bruker MSL-300 spectrometer. The ^{27}Al resonance frequency was 104.26 MHz and the rotor was spun at 4.5 kHz. The radio frequency field was 5.0 kHz corresponding to a pulse width of 5 μs, and the recycle time was 2 s with a delay of 10 μs. The samples were in equilibrium with a saturated vapor of a mixture of 1 : 1 (volume ratio) acetyl acetone and 95% ethyl alcohol for 8 days at room temperature. $AlCl_3 \cdot 6H_2O$ was used as the external reference for aluminum. XPS spectra were recorded on a Perkin-Elmer PHI-5000C ESCA system with Al$K\alpha$ radiation. A binding energy of 284.6 eV for the C_{1s} level was used as an internal reference for all the samples. Microcalorimetric studies of the adsorption of NH_3 were carried out at 150°C using a Tian-Calvet type heat-flux calorimeter. The catalysts were evacuated at 250°C for 3 h before measurements. A chemical method was used for the detection of sulfate content of the samples. Dehydrated Na_2CO_3 and ZnO (1 : 4) were used as fusing agents, and the sulfate was turned into $BaSO_4$ and determined by gravimetric method.

The isomerization of *n*-butane was performed at 35°C in a closed reaction system. Catalyst (0.5 g) was placed in the reactor and 5 ml (S.T.P.) of 99.9% pure *n*-butane was injected for each test. The *n*-butane reaction at 250°C was carried out in a flow-type fixed bed reactor under ambient pressure. Catalyst (1.0 g) was loaded, and a mixture of butane (*n*-butane : isobutane = 4 : 1) and H_2 (1 : 10 molar ratio) was fed at a rate of WHSV 0.3 h^{-1}. The *n*-pentane reaction was run in a pulsed microreactor under ambient pressure. Catalyst (0.1 g) was loaded, and the carrier gas was N_2 with a flow rate of 30 ml min^{-1}. The amount of *n*-pentane injected for each pulse was 0.5 μl. Benzoylation of toluene was carried out in a three-necked round-bottom flask fitted with a reflux condenser. Benzoyl chloride (1 mL), 20 mL toluene, and 0.5 g catalyst were added into the flask and heated at 110°C. The HCl effluent gas was absorbed by a NaOH solution. The products of the above reactions were analyzed by a gas chromatograph equipped with FID. The yield of methylbenzophenone was based on the amount of benzoyl chloride added into the reaction.

RESULTS

Effect of Al on Crystallization

It is well known that the dried sulfated zirconia must be calcined at elevated temperature to produce strong acidity. An appropriate calcination temperature ranges from 600 to 650°C. XRD patterns of sulfated zirconia and Al-promoted sulfated zirconia catalysts calcined at 650°C for 3 h are shown in Fig. 1. It can be seen that a small amount of monoclinic ZrO_2 phase is presented in SZ along with the tetragonal ZrO_2 phase. For SZA catalysts only the tetragonal phase exists, indicating that the transformation from the metastable tetragonal phase to the monoclinic phase is retarded in the presence of Al. It is interesting to note that the intensity of the characteristic diffractive peaks of the tetragonal phase increases slightly with Al_2O_3 content up to 6.0 mol% and then decreases gradually as the Al_2O_3 content is further increased. SZA catalysts containing 15.0 mol% or more Al_2O_3 begin to crystalline above 700°C, and only tetragonal phase is observed at 750°C. This shows that the crystallization of amorphous zirconium dioxide to form tetragonal zirconia is also sensitive to the Al content of the sample. The addition of a small amount of Al_2O_3 enhances the crystallization of the tetragonal phase.

XRD patterns of the STA and SFA series samples are shown in Figs. 2 and 3, respectively. After calcining at 500°C

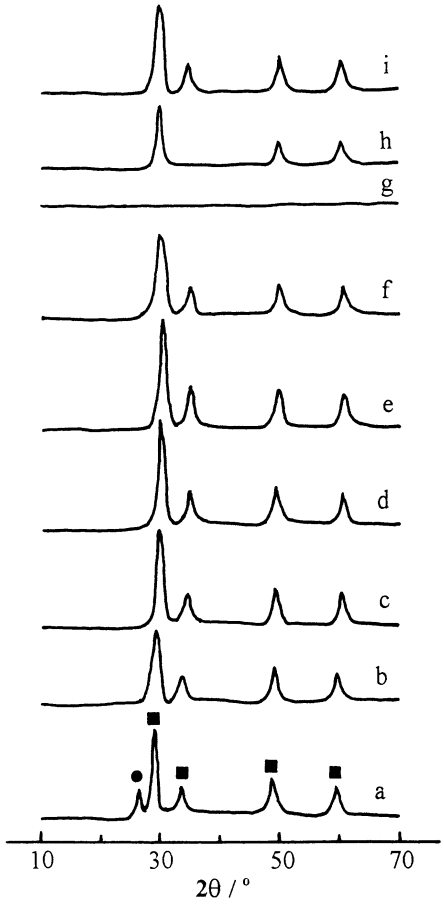

FIG. 1. XRD patterns of various SZA samples: (a) SZ (650°C), (b) SZA-1 (650°C), (c) SZA-2 (650°C), (d) SZA-3 (650°C), (e) SZA-4 (650°C), (f) SZA-5 (650°C), (g) SZA-6 (650°C), (h) SZA-6 (700°C), (i) SZA-6 (750°C). (●) Monoclinic phase, (■) tetragonal phase.

for 3 h, the anatase phase and α-Fe_2O_3 phase are observed in ST and SF samples, respectively. For STA and SFA catalysts the intensity of the characteristic diffractive peaks of these crystalline phases changes with the Al_2O_3 content in a way similar to that of the tetragonal ZrO_2. It increases slightly with Al_2O_3 content up to 3.0 mol% and then decreases slightly as the Al_2O_3 content is further increased.

For the above three series Al-promoted catalysts, there are no characteristic peaks of Al_2O_3 in the patterns, implying that Al_2O_3 is sufficiently homogeneously mixed with zirconia, titania, and iron oxide. On the contrary, after calcining at 650°C, a typical γ-Al_2O_3 phase is observed in SA sample, and the pattern of SγA sample reveals some different Al_2O_3 phases, such as γ-, η-, and α-Al_2O_3.

Our previous work on sulfated zirconia showed that there is some relation between the crystallographic phase of ZrO_2 and the strong acidity and catalytic activity of the catalysts (13). In general, sulfated samples with a more stable tetragonal crystalline structure possess more strong acid sites and higher activity for *n*-butane isomerization. The relationship between the crystal phase of ZrO_2 and the catalytic activity of these samples have also been reported by various others. Early investigations suggested that the tetragonal ZrO_2 phase is essential for producing a superacidic material (22, 23). Later other authors demonstrated that a stable tetragonal ZrO_2 phase is a necessary structural condition for obtaining samples active in the isomerization of *n*-alkanes, and meanwhile sulfated monoclinic ZrO_2 phase is catalytically inert for the reaction (24). Recently, Stichert and Schuth reported that the activity of sulfated monoclinic zirconia for *n*-butane isomerization given in $mol\,s^{-1}\,m^{-2}$ is lower than that of sulfated tetragonal zirconia, but the monoclinic sample is still reasonably active for the reaction (25). Based on all these observations, it can be suggested that the promotion of the crystallization of tetragonal ZrO_2, anatase, and α-Fe_2O_3 and the retardation of the phase transformation of ZrO_2 from tetragonal to monoclinic for the Al-promoted samples are probably a part of the factors causing an enhancement in their acidity and catalytic activity.

TG-DTG Analysis

The TG-DTG profiles of some typical uncalcined samples are depicted in Fig. 4. There is a quick weight loss peak at 75–110°C in all the samples, corresponding to the desorption of water. In the meanwhile, a high-temperature weight

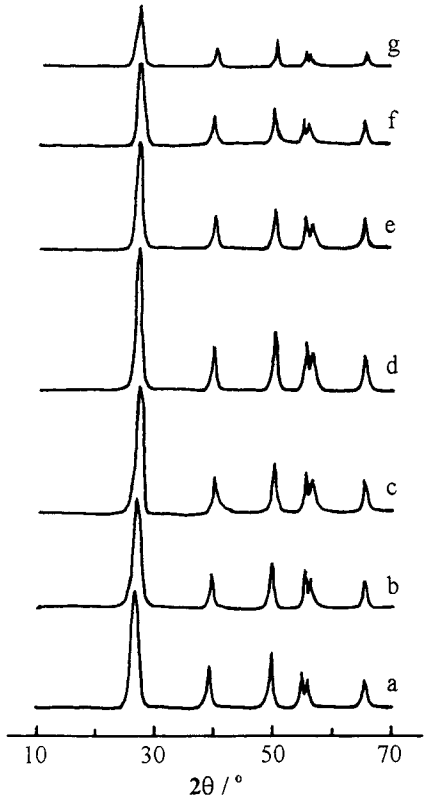

FIG. 2. XRD patterns of STA samples with different Al_2O_3 content calcined at 500°C: (a) ST, (b) STA-1, (c) STA-2, (d) STA-3, (e) STA-4, (f) STA-5, (g) STA-6.

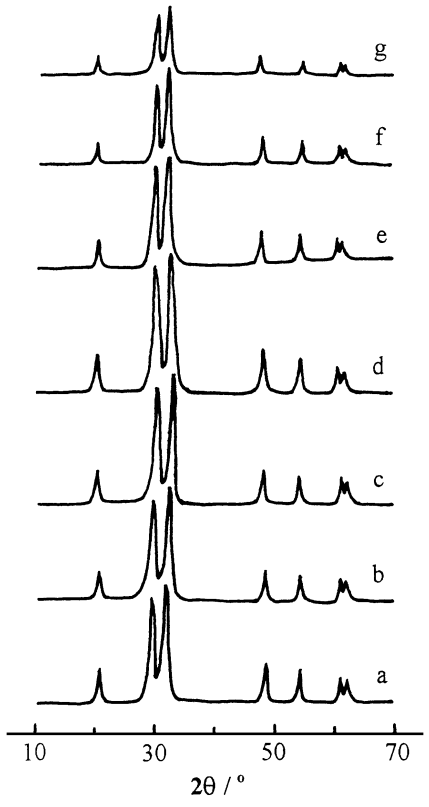

FIG. 3. XRD patterns of SFA samples with different Al_2O_3 content calcined at 500°C: (a) SF, (b) SFA-1, (c) SFA-2, (d) SFA-3, (e) SFA-4, (f) SFA-5, (g) SFA-6.

loss peak is also observed, which may correspond to the decomposition of sulfate species in the samples. The temperature of the latter peak depends on the nature of metal oxides and the amount of Al_2O_3 loading in the materials. For SZ and SZA-3 samples, a shoulder peak is observed beside this high-temperature weight loss peak, showing that sulfated species with different thermal stability are present in the samples. The high-temperature weight loss peak of SZA-3 containing 3.0 mol% Al_2O_3 shifts to 755°C, which is 40°C higher than that of SZ. For STA-2 and SFA-2 samples, containing 1.5 mol% Al_2O_3, the high-temperature weight loss peaks appeared at 598 and 596°C, which are also 38 and 6°C higher than those of ST and SF catalysts, respectively. The shift of the high-temperature weight loss peak to higher temperatures for the Al-promoted catalysts indicates an increase in the thermal stability of the surface sulfate species in these samples. For this type of catalysts the sulfated oxides must be calcined in air at 500–650°C to form surface sulfate complexes on the catalysts and sometimes the catalysts are pretreated *in situ* at 250–400°C again before reaction, so the higher thermal stability of the surface sulfate species in the Al-promoted catalysts reduces the unavoidable sulfate loss during preparation and pretreatment, which is indeed of advantage to increase the acidity and activity of the catalysts.

Surface Area and Sulfate Content

The surface area and sulfate content of all the catalysts calcined at designated temperatures are presented in Table 1. In a certain range of Al_2O_3 incorporated, the surface area of the three series samples increases with Al_2O_3 content. The increase in surface area is more eminent for STA and SFA than for SZA series catalysts. In the meantime, the SO_3 content of SZA, STA, and SFA catalysts increases significantly with Al_2O_3 content. The surface area and SO_3 content of SZA-6 are evidently lower than those of all the other SZA catalysts, because its calcination temperature has been raised to 750°C for ZrO_2 in the catalyst to crystallize. The above results show that the incorporation of Al is advantageous in increasing both the surface area and the surface concentration of sulfate species for the three series of catalysts. Although the nature of the surface sulfate species is important rather than the sulfur content, for the same series of catalysts an abundance of surface sulfate species may correspond to an increase in surface active sites. SA and SγA have only weak acid sites, but both of them have a high sulfate content. The surface area of SγA is nearly two times smaller than that of SA, so its surface concentration of sulfate species is much higher than that of SA. This shows that the concentration of sulfate species of the catalysts depends on the crystal structure of the oxide.

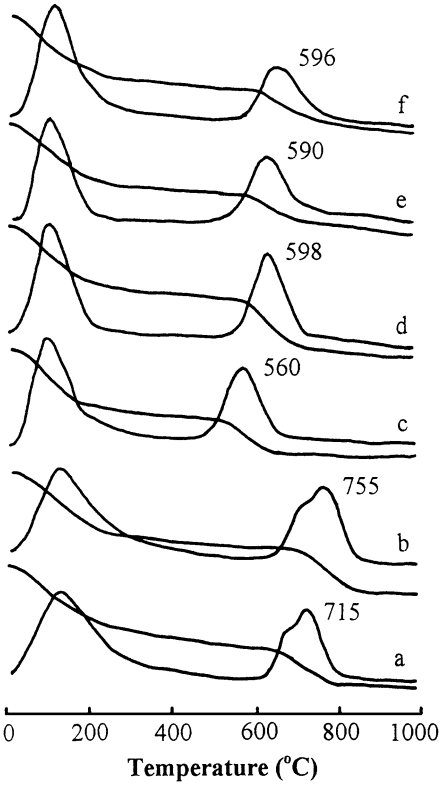

FIG. 4. TG-DTG profiles of (a) SZ, (b) SZA-3, (c) ST, (d) STA-2, (e) SF, (f) SFA-2.

TABLE 1

Surface Area and Sulfur Content of Various Samples

Sample	Al_2O_3 content (mol%)	Calcination temp. (°C)	Surface area (m^2/g)	SO_3 content (μmol/g)
SZ	0	650	113.0	412
SZA-1	0.5	650	123.6	587
SZA-2	1.5	650	126.3	612
SZA-3	3.0	650	139.8	800
SZA-4	6.0	650	135.2	875
SZA-5	10.0	650	132.8	975
SZA-6	15.0	750	104.3	487
ST	0	500	114.1	642
STA-1	0.5	500	121.0	651
STA-2	1.5	500	135.6	753
STA-3	3.0	500	147.3	1017
STA-4	6.0	500	192.7	1180
STA-5	10.0	500	192.2	1194
STA-6	15.0	500	176.6	1369
SF	0	500	63.7	502
SFA-1	0.5	500	65.0	514
SFA-2	1.5	500	68.6	525
SFA-3	3.0	500	72.3	566
SFA-4	6.0	500	78.1	659
SFA-5	10.0	500	105.4	821
SFA-6	15.0	500	115.6	915
SA	100	650	296.9	1052
SγA	100	650	91.5	1933
SZFM	0	650	105.0	524

It seems that the denser α-Al_2O_3 structure with six coordinated Al^{3+} has a higher sulfate accommodation ability than the γ-Al_2O_3 structure with both six and four coordinated Al^{3+}.

XPS and ^{27}Al MAS NMR

XPS spectra of several typical catalysts show that the binding energies of S($2p_{3/2}$), Zr($3d_{5/2}$), Ti($2p_{3/2}$), and Fe($2p_{3/2}$) are essentially unaltered, implying that these elements in the catalysts remain in the valence state of S^{6+}, Zr^{4+}, Ti^{4+}, and Fe^{3+}. the surface atomic ratio of three typical Al-promoted samples was obtained by XPS and presented in Table 2. The surface atomic ratio Al/M (M = Zr, Ti, Fe) of SZA-3, STA-2, and SFA-2 catalysts is 0.201, 0.074, and 0.099, respectively, which is two to six times the bulk atomic ratio of the relevant catalysts, indicating that the surface of all these Al-promoted samples is rich in Al. The distinct

TABLE 2

Atomic Ratio of Al-Promoted Samples

Sample	Al/M ratio in bulk[a]	Al/M ratio in surface[a]
SZA-3	0.061	0.201
STA-2	0.030	0.074
SFA-2	0.015	0.099

[a] M = Zr, Ti, and Fe.

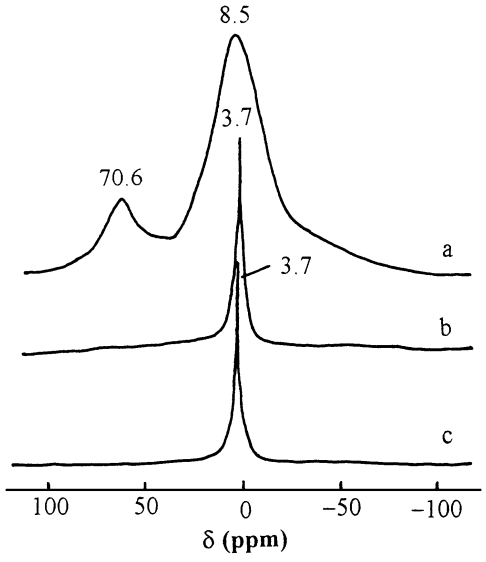

FIG. 5. ^{27}Al MAS NMR spectra of (a) SA, (b) STA-2, (c) SZA-3.

enrichment in Al corresponds to an abundance of Al−O−M bonds on the surface, which may facilitate the accommodation of surface sulfate species and generate more strong acid sites.

^{27}Al MAS NMR spectra of some of the Al-promoted samples and SA are shown in Fig. 5. On the spectra of SZA-3 and STA-2, only a sharp octahedral Al peak (3.7 ppm) is observed, showing that Al is probably located in the crystal lattice of ZrO_2 and TiO_2 forming isomorphs or solid solutions. However, on the spectrum of SA in addition to a large peak of octahedral Al (8.5 ppm) a smaller tetrahedral Al peak (70.6 ppm) is present, corresponding to the two coordination states of Al in γ-Al_2O_3 crystal structure. The above results are consistent with those of XRD.

Acidity Measurements

A variety of techniques have been used to measure the acidity of sulfated oxide catalysts, but it seems that some techniques widely used in the characterization of other solid acid catalysts are not suitable for these types of catalysts. For example, temperature-programmed desorption of NH_3, pyridine, and benzene may give incorrect results on acid strength distribution due to the oxidative decomposition of adsorbate molecules at elevated temperature (26–28). Infrared spectra of pyridine adsorbed on acid catalysts were often used to measure Brønsted and Lewis acidity. However, it has been found recently that Lewis acidity calculated on the basis of pyridine adsorption spectra of sulfated oxide systems is overestimated due to a ligand-displacement effect between pyridine and sulfates on the surface of the sample (29). Most authors agree that both Lewis and Brønsted acid sites exist on sulfated oxide catalysts, but the role of the two types of acidity in alkane isomerization or other reactions still gives rise to much controversy (14, 30). In

TABLE 3

Stretching Frequency, Bond Order, and Partial Charge on Oxygen of S=O before and after Water Adsorption

	SO stretching frequency (cm^{-1})			Bond order		Partial charge on oxygen	
Sample	B[a]	A[b]	Shift	B	A	B	A
SZ	1392	1352	40	1.87	1.80	−0.13	−0.20
SZA-2	1383	1342	41	1.85	1.79	−0.15	−0.21
SZA-3	1384	1342	42	1.85	1.79	−0.15	−0.21
SZA-4	1392	1351	41	1.87	1.80	−0.13	−0.15
ST	1369	1347	22	1.83	1.79	−0.17	−0.21
STA-1	1369	1347	22	1.83	1.79	−0.17	−0.21
STA-2	1369	1345	24	1.83	1.79	−0.17	−0.21
STA-3	1381	1357	24	1.85	1.81	−0.15	−0.19
SF	1370	1355	15	1.83	1.81	−0.17	−0.19
SFA-2	1367	1351	16	1.82	1.80	−0.18	−0.20

[a] Before water adsorption.
[b] After water adsorption.

this work the relative acid strength of the sulfated oxide catalysts was detected by an infrared spectroscopic method (31), and microcalorimetry was employed to measure the heats of ammonia adsorption to determine the number and acid strength distribution of the acid sites on the catalysts.

Infrared spectra of the catalysts after evacuation at 350°C for 3 h display a strong band at 1367–1392 cm^{-1}, characteristic of the surface sulfate species having covalent S=O bonds (32). When water is adsorbed on the surface sulfate, a red shift of this IR band is observed, indicating a strong interaction between the adsorbed water molecules and the surface sulfate species. This frequency shift corresponding to a decrease in the bond order of S=O covalent bond and an increase in the partial charge on oxygen atom increases with the acid strength of the catalyst (31). The S=O stretching frequency, the bond order and partial charge on oxygen atom calculated according to equations in the literature (32, 33) for some of the catalysts are listed in Table 3. The S=O frequency shifts of the three series of catalysts are in the order of SZ, SZA > ST, STA > SF, SFA, indicating that the relative acid strength of the catalysts decreases in the same sequence. On the other hand, in the same series of catalysts, the frequency shifts of the Al-promoted catalysts are almost identical with those of the respective unpromoted catalysts, implying that the incorporation of aluminum has little effect on the relative acid strength of the catalysts.

The catalysts were evacuated at 250°C for 3 h before microcalorimetric measurements. Figure 6 shows the microcalorimetric results of NH_3 adsorption at 150°C on the catalysts. The differential heat of adsorption decreases with increasing NH_3 coverage, indicating that the acid sites in the catalysts are not homogeneous (34). The initial adsorption heats of NH_3 on the strong acid sites for the Al-promoted catalysts are nearly the same as those for the respective unpromoted catalysts. For SZ and SZA-3, ST and STA-2, and SF and SFA-2, the initial adsorption heats are 170 kJ mol^{-1}, 160 kJ mol^{-1}, and 150 kJ mol^{-1}, respectively. Histograms and data of the distribution of acid site strengths are shown in Figs. 7–9 and Table 4. The distribution of acid sites is greatly changed when introducing a small amount of Al_2O_3 into the catalysts. The number of weak acid sites with differential heats between 80 and 125 kJ mol^{-1} on all the Al-promoted catalysts is lower than that on the respective unpromoted catalysts, but the number of intermediate–strong acid sites with differential heats between 125 and 140 kJ mol^{-1} is significantly higher than that on the respective unpromoted catalysts. The acid strengths of the acid sites on SZ are more evenly distributed, whereas SZA-3 possesses a greater number of intermediate–strong acid sites with differential heats between 125 and 140 kJ mol^{-1}. The number of acid sites with differential heats in the range of 125 to 140 kJ mol^{-1} for SZA-3 is 4.3 times greater than that for SZ.

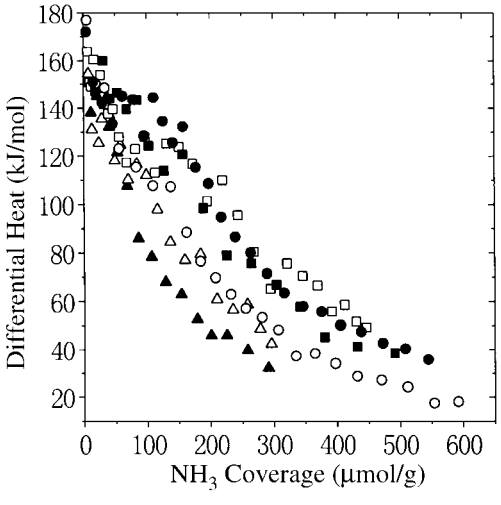

FIG. 6. Differential heat of NH_3 adsorption versus adsorption coverage for (○) SZ, (●) SZA-3, (□) ST, (■) STA-2, (△) SF, (▲) SFA-2.

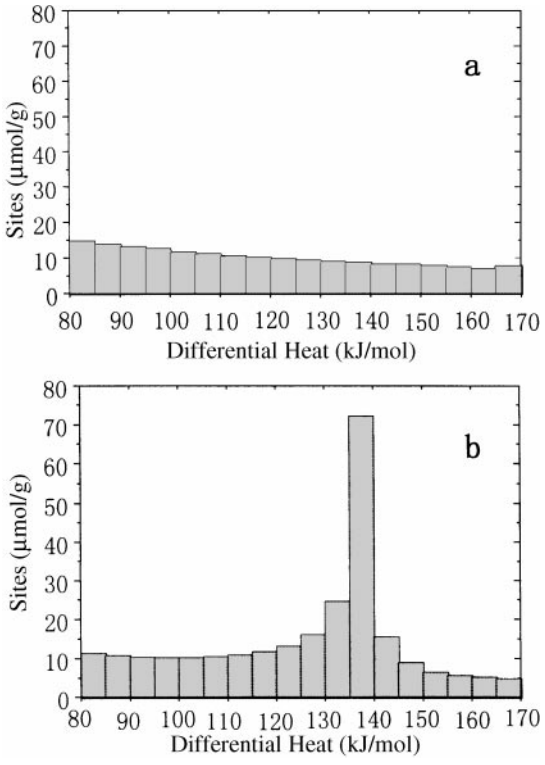

FIG. 7. Histograms of acid strength distributions for (a) SZ and (b) SZA-3 catalysts.

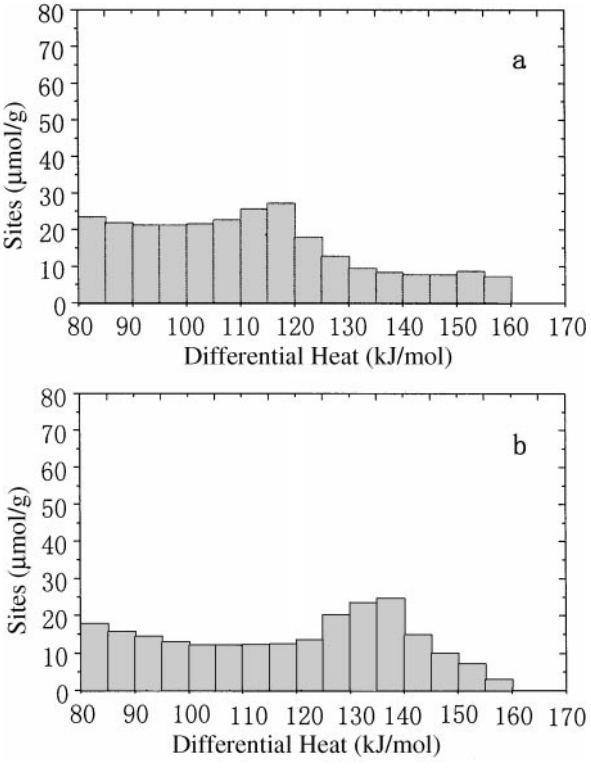

FIG. 8. Histograms of acid strength distributions for (a) ST and (b) STA-2 catalysts.

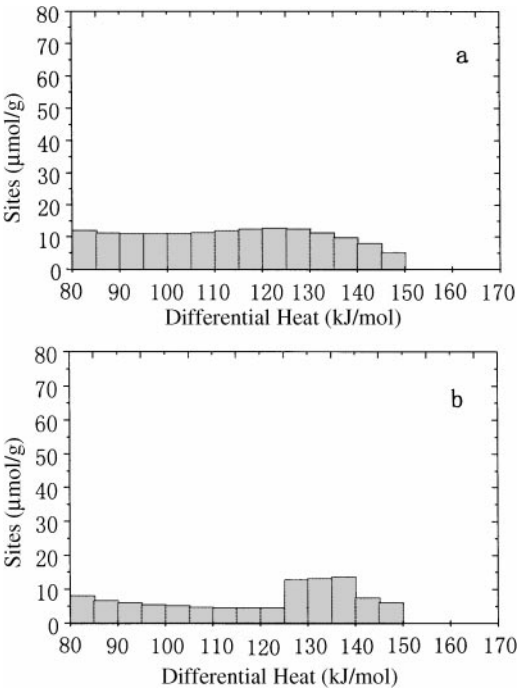

FIG. 9. Histograms of acid strength distributions for (a) SF and (b) SFA-2 catalysts.

The data in the parentheses in Table 4 are the number of acid sites of mixtures of SZ, ST, or SF and SA with the same molar ratio of ZrO_2/Al_2O_3, TiO_2/Al_2O_3, or Fe_2O_3/Al_2O_3 as that in SZA-3, STA-2, or SFA-2 catalysts. It is obvious that the number and acid strength distribution of the acid sites of the mixtures are close to those of the unpromoted catalysts numerically. Hence, the change in the number and acid strength distribution of the acid sites of the Al-promoted catalysts could be related to a strong interaction of the Al atoms with the metal oxides. In the studies of zirconia-doped alumina it has been observed that Zr is incorporated into the lattice structure of alumina through

TABLE 4

Microcalorimetric Results of the Distribution of Acid Site Strengths

Catalyst	Acid sites (μmol/g)			
	Total	80–125 kJ/mol	125–140 kJ/mol	140–170 kJ/mol
SZ	178.2	106.1	26.4	45.7
SZA-3[a]	259.1 (183.6)	99.4 (111.1)	113.0 (27.6)	46.7 (44.9)
ST	265.0	203.2	30.6	31.2
STA-2[b]	226.1 (267.5)	122.9 (205.2)	68.3 (31.4)	34.9 (30.9)
SF	151.5	104.5	33.7	13.3
SFA-2[b]	100.1 (153.8)	49.8 (106.4)	36.7 (34.1)	13.6 (13.4)

[a] Data in the parentheses are numbers of acid sites of mixture of SZ and SA with ZrO_2/Al_2O_3 molar ratio of 97/3.

[b] Data in the parentheses are numbers of acid sites of mixture of ST or SF and SA with TiO_2/Al_2O_3 or Fe_2O_3/Al_2O_3 molar ratio of 98.5/1.5.

Al–O–Zr bonding (35, 36). The formation of Al–O–Zr and Al–O–Ti bonds in the binary oxides is probably responsible for the observed enhancement in the amount of intermediate strong acid sites for the Al-promoted catalysts.

Catalytic Test

Isomerization of *n*-butane and *n*-pentane and benzoylation of toluene with benzoyl chloride are used as gas and liquid phase strong acid catalyzed reactions to test the catalytic activity of the catalysts.

The isomerization of *n*-butane was run at 35°C in a closed reactor system. At ambient temperature the reaction proceeds only on superacidic or strong acid sites of the catalysts and it follows the rate law of a first-order reversible reaction (37). Therefore, catalytic activity expressed in the terms of the forward and backward rate constants k_1 and k_{-1} is associated with the strong acidity of the catalysts. The activities of the catalysts expressed in terms of *n*-butane conversion after being on stream for 20 h or the calculated rate constants of the reaction are listed in Table 5. For the unpromoted catalysts, the isomerization activity of the catalysts is in the order of SZFM > SZ > ST > SF > SγA, SA. For the Al-promoted catalysts, the isomerization activity increases with Al_2O_3 content up to a maximum and then decreases as the Al_2O_3 content is further increased. The variation of activity with Al_2O_3 content for the three series of catalysts is shown in Fig. 10. The activities of the three series of catalysts are in the order of SZA > STA > SFA. It is obvious that the activity data in Table 5 do not coincide with the SO_3 content data in Table 1, implying that not all surface sulfate species on the catalysts are acid sites which are strong enough to be active for *n*-butane isomerization at ambient temperature. This phenomenon is consistent with the results of microcalorimetric measurements.

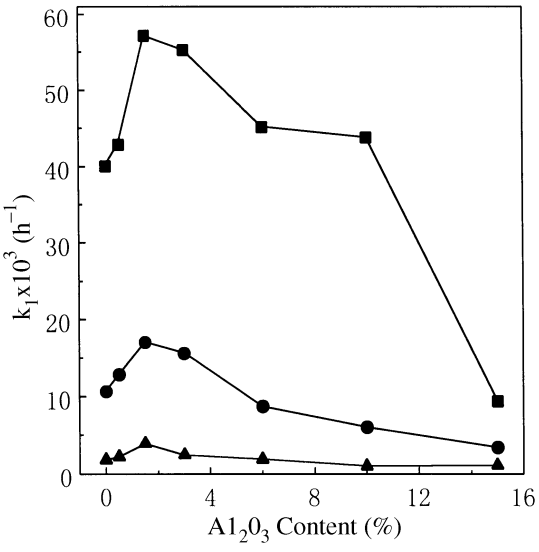

FIG. 10. Variation of *n*-butane isomerization activity with Al_2O_3 content: (■) SZA series, (●) STA series, (▲) SFA series.

The isomerization of *n*-butane was carried out at 250°C in a flow reactor as well. The major reaction product is isobutane, and the main by-products are propane and isopentane. The selectivity to isobutane for all the catalysts is above 95%. The variation of the conversion of *n*-butane with time on stream for SZ, SZA, and SZFM catalysts is given in Table 6. The ST and SF series catalysts are almost inactive for the reaction under the same conditions. The initial conversion of SZ is the highest, but it decreases rapidly with time on stream. The steady-state conversion of SZ is reduced by more than three times. The initial conversion of SZFM is lower than that of SZ and it deactivates even

TABLE 5

Kinetic Data for *n*-Butane Isomerization at 35°C

Sample	Conversion[a] (%)	k_1 (10^{-3} h^{-1})	k_{-1} (10^{-3} h^{-1})
SZ	37.10	40.1	12.81
SZA-1	48.23	41.0	13.09
SZA-2	56.66	57.2	18.27
SZA-3	51.50	55.3	17.67
SZA-4	49.71	45.2	14.44
SZA-5	46.41	41.8	13.35
SZA-6	15.12	9.40	3.00
ST	15.60	10.67	3.41
STA-1	20.14	12.84	4.10
STA-2	29.74	16.06	5.13
STA-3	25.58	15.62	4.99
STA-4	9.18	8.75	2.80
STA-5	7.46	7.07	2.26
STA-6	3.22	3.42	1.09
SF	5.59	2.20	0.71
SFA-1	7.20	2.45	0.79
SFA-2	9.58	3.13	1.00
SFA-3	4.74	2.41	0.77
SFA-4	3.11	1.47	0.47
SFA-5	2.54	1.37	0.44
SFA-6	2.19	1.08	0.35
SA[b]	0.24	0.25	0.14
SγA[b]	0.69	0.59	0.33
SZFM	72.4	134.8	43.1

[a] Conversions obtained after on stream for 20 h.
[b] The reaction temperature is 75°C.

TABLE 6

***n*-Butane Isomerization at 250°C**

Catalyst	Conversion (%)					
	2 min	10 min	60 min	120 min	180 min	360 min
SZ	38.6	30.0	15.4	12.1	11.8	11.5
SZA-2	26.0	24.0	21.0	20.0	19.0	19.0
SZA-3[a]	28.0	27.0	26.5	25.0	25.0	25.0
SZA-4	27.5	24.6	19.9	19.5	19.1	19.1
SZFM	26.1	13.3	1.5	—	—	—

[a] The conversion of SZA-3 after on stream for 120 h remains at 25.0%.

more rapidly than SZ. It is interesting to note that all the SZA catalysts deactivate much more slowly than the others. The steady-state conversion of SZA-3 is 25%, which is 2.2 times higher than that of SZ. Since our original reactant contains 20% isobutane, the actual concentration of isobutane in the reaction product is 45%, which means that the isomerization of *n*-butane proceeds on SZA-3 catalyst steadily at a level of 88% of the thermodynamic equilibrium. Comparing with all the other sulfated oxide-based catalysts reported in the literature, the higher activity and exceptional stability of SZA are unique, which is indeed advantageous in the practical point of view.

The catalytic activity and stability of the catalysts for *n*-pentane isomerization were tested at 300°C, using a pulsed microreactor. The major reaction products are isopentane and isobutane, and the minor products are *n*-butane, propane, and traces of hexane. The variation of *n*-pentane conversion with pulse number of SZ, SZA-3, and SZFM is shown in Fig. 11. The ST and SF series catalysts are almost inactive for this reaction as well. The initial conversion of the catalysts is in the order of SZA-3 > SZ > SZFM, and the steady-state conversion of the catalysts is in the same order. Both SZ and SZFM deactivate rapidly in this reaction, whereas the steady state conversion of SZA-3 remains at a high level of 69%. The above results show again that the Al-promoted sulfated zirconia catalyst is more active and stable than the unpromoted and transition metal promoted catalysts in *n*-pentane isomerization as well as in *n*-butane isomerization.

Friedal Crafts acylation of aromatics is an important reaction in organic synthesis. Benzoylation of toluene with benzoyl chloride was used as a test reaction to investigate the catalytic activity of the samples for this type of liquid acid-catalyzed reactions. The product of the heterogeneous benzolyation of toluene with benzoyl chloride on our catalysts is a mixture of *p*-, *o*-, and *m*-methylbenzophenone, and the proportions of the isomers are in the range of *p*-methylbenzophenone 62–71%, *o*-methylbenzophenone 28–35%, and *m*-methylbenzophenone 1–3%. The yields

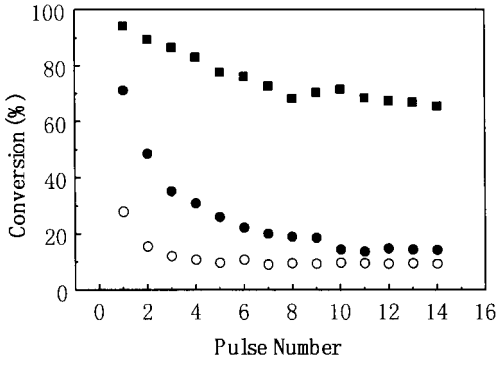

FIG. 11. Variation of *n*-pentane conversion with pulse number: (■) SZA-3, (●) SZ, (○) SZFM.

TABLE 7

Catalytic Activities for the Benzoylation of Toluene with Benzoyl Chloride

Sample	Yield (%)					
	1 h	2 h	4 h	6 h	8 h	10 h
SZ	22.98	32.84	46.89	59.53	65.98	70.92
SZA-1	24.95	35.47	57.18	72.02	81.84	85.93
SZA-2	28.5	38.38	57.45	73.14	82.65	88.6
SZA-3	39.67	58.74	75.26	84.34	89.55	91.22
SZA-4	26.4	37.1	49.17	61.34	69.71	79.18
SZA-5	21.33	29.51	40.78	50.25	61.37	72.35
SZA-6	19.62	24.96	32.45	38.99	45.03	48.54
ST	19.45	24.39	29.73	34.83	38.42	41.72
STA-1	19.63	24.61	32.43	39.55	44.62	48.45
STA-2	23.17	30.58	37.63	45.61	50.46	55.30
STA-3	19.53	24.96	31.91	37.50	41.91	44.72
STA-4	19.84	23.68	29.86	35.43	40.24	42.58
STA-5	18.28	21.41	25.52	30.89	36.77	39.49
STA-6	17.45	21.32	27.28	32.28	36.10	38.26
SF	48.83	56.98	63.76	69.38	73.50	77.13
SFA-1	48.21	58.30	66.00	71.64	76.12	79.19
SFA-2	51.86	64.11	71.73	76.38	80.75	83.65
SFA-3	48.80	57.84	64.20	70.47	74.41	78.08
SFA-4	46.18	57.44	64.51	69.69	74.15	77.18
SFA-5	46.02	55.05	63.93	69.06	73.59	76.92
SFA-6	46.34	57.19	64.94	69.12	73.05	76.64
SA	5.42	6.80	10.41	14.89	18.17	21.81
SγA	15.31	18.84	25.04	28.45	33.54	38.48

of methylbenzophenones on SZA, STA, and SFA series catalysts containing different amount of Al_2O_3 at 110°C are compared in Table 7. The yield of methylbenzophenones increases with reaction time. The catalytic activity of the unpromoted catalysts is in the order of SF > SZ >

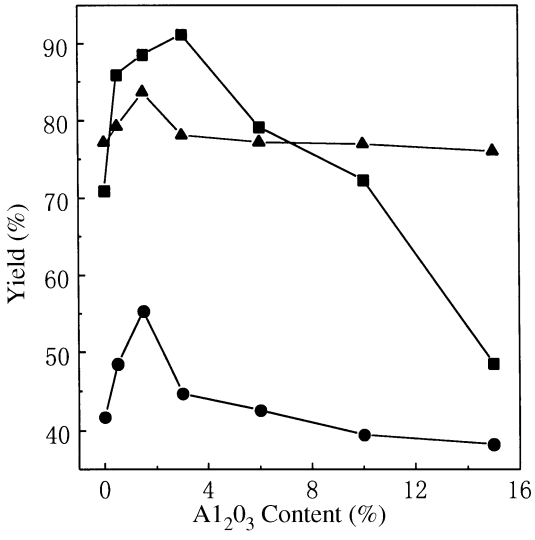

FIG. 12. Variation of the yield of methylbenzophenones after 10 h on stream with Al_2O_3 content: (■) SZA series, (●) STA series, (▲) SFA series.

ST > SγA > SA. For the Al-promoted catalysts, the variation of the yield of methylbenzophenones after being on stream for 10 h with Al_2O_3 content is shown in Fig. 12. Similar to the results of *n*-butane isomerization, the catalytic activity increases with Al_2O_3 content up to a maximum and then decreases as the Al_2O_3 content is further increased. The activities of the three series of catalysts are in the order of SZA > SFA > STA. The extraordinary high activities of SF and SFA catalysts toward this reaction are consistent with results of Arata *et al.* (38, 39). It was explained that iron chloride was formed on the catalyst surface because of the probable reaction of benzoyl chloride or HCl evolved in the reaction with the iron component in the catalyst.

DISCUSSION

The addition of transition metal (e.g., Fe, Mn, Cr, V, etc.) oxides has been found to increase the acidity and activity of sulfated zirconia catalysts for *n*-butane isomerization (7, 12). Early investigations suggested that the presence of these transition metal oxide promoters increases both the number and the strength of the acid sites on SZ. Recently, more and more authors believe that the reason for the high activity of the transition metal-promoted catalysts is an increased formation of butene owing to the dehydrogenation reactivity of the promoters. The isomerization of *n*-butane on SZ-based catalysts proceeds through a bimolecular mechanism as shown in the following scheme (40, 41):

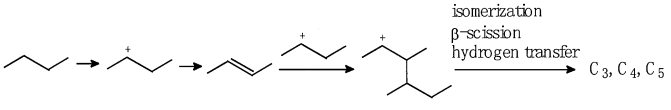

SCHEME 1

The increased formation of butene will no doubt accelerate the reaction. However, *n*-C_4 olefins are also the primary species responsible for deactivation of the catalysts by coking during *n*-butane isomerization (30), so that the transitional metal promoted SZ catalysts deactivate even more rapidly than the unpromoted catalysts. The exceptionally high activity of transition metal-promoted SZs makes them very attractive as catalysts for hydrocarbon conversion and other reactions, but the rapid deactivation is an inherent drawback of these types of catalysts. Therefore, studies on the promoting effect of main group elements on sulfated zirconia had been initiated in our laboratory. In consequence, we found that Al is a very good promoter for sulfated zirconia, titania, and iron oxide. The addition of Al increases the activity of the sulfated oxide catalysts for isomerization of *n*-butane and *n*-pentane in gas phase and benzoylation of toluene with benzoyl chloride in liquid phase significantly. In particular, the stability of the Al-promoted catalysts in the isomerization reaction of *n*-alkanes is improved. Under 250°C *n*-butane isomerization can proceed on Al-promoted sulfated zirconia at a level of 88% of thermodynamic equilibrium conversion continuously without observable deactivation. The unique catalytic performance of the Al-promoted sulfated zirconia in *n*-alkane isomerization makes it superior to other sulfated oxide catalysts including transition metal-promoted sulfated zirconia catalysts, such as the well known SZFM.

Microcalorimetric measurements of the adsorption of ammonia can be used to measure the number and acid strength distribution of the acid sites on solid acid catalysts quantitatively (42). Results of microcalorimetric measurements of the Al-promoted catalysts show that the number of acid sites with intermediate acid strength, having differential heats of NH_3 adsorption in the range of 125–140 kJ mol^{-1}, is increased as compared with the unpromoted catalysts especially in the case of SZA. The effect of acid strength on the activity and deactivation of sulfated zirconia catalysts has been studied by kinetic measurements of *n*-butane isomerization over catalysts selectively poisoned with ammonia (42). It has been observed that though acid sites with heats of 125–140 kJ mol^{-1} do not show initial high activity, these sites contribute to long-term catalytic activity. Thus, the increased amount of acid sites with intermediate acid strengths over the Al-promoted catalysts is probably responsible for their high catalytic activity and slow deactivation in *n*-alkane isomerization reactions and other acid-catalyzed reactions.

Since the promoting effect of Al is related to an increase in the number of catalytic sites with intermediate acid strengths, it would be of interest to examine various factors influencing the enhancement of these surface acid sites on the Al-promoted catalysts. XRD and XPS studies of the catalysts show that the promotor Al^{3+} is probably located in the crystal lattice of zirconia and titania forming isomorphs or solid solutions, and it is six coordinated. The surface enrichment in Al and the formation of Al–O–Zr and Al–O–Ti bonds on the surface of the Al-promoted catalysts are probably the causes for the enhancement in the amount of intermediate strong acid sites. According to the principle of electronegativity equalization proposed by Sanderson (43), since the electronegativity of Al^{3+} is larger than that of Zr^{4+} and Ti^{4+}, the positive charge on Zr and Ti atoms is increased due to the formation of Al–O–Zr and Al–O–Ti bonds, which generates stronger acidity on these sites. At the same time, the charge transfer from Zr and Ti atoms to the neighboring Al atoms strengthens the Al–O bond between Al and the surface sulfate species. The stronger Al–O bond leads to an increase in the thermal stability of the surface sulfate species and in consequence the acidity of the catalysts is enhanced.

In summary, this work shows that a main group element, such as Al, has been used successfully as a promotor to improve the catalytic performance of sulfated oxide catalysts. The promoting effect of Al is different from that of transition metals. The formation of Al–O–Zr and Al–O–Ti bonds in the oxides leads to an enhancement in the number of intermediate strong acid sites on the promoted catalysts and improves the activity and stability of the catalysts for *n*-alkane isomerization and other acid-catalyzed reactions.

CONCLUSIONS

It is found that the main group element Al is a good promoter for sulfated oxide catalyst systems. Introducing a small amount of Al_2O_3 into sulfated zirconia, titania, and iron oxide enhances their activity for *n*-alkane isomerization and benzoylation of toluene with benzoyl chloride considerably. In particular, the catalytic stability of Al-promoted sulfated zirconia in *n*-alkane isomerization is improved significantly as compared with the unpromoted or transition metal promoted catalysts. The promoting mechanism of Al is different from that of the transition metals. The enhanced long-term activity of the Al-promoted catalysts is associated with an increase in intermediate strong acid sites on the catalysts, which is caused by the formation of Al–O–Zr and Al–O–Ti bonds in the mixed oxides. The strong Al–O–Zr and Al–O–Ti bonds lead to an increase in the concentration and thermal stability of the surface sulfate species and generate additional acidic active sites for the reactions.

ACKNOWLEDGMENT

This work was financially supported by The State Science and Technology Commission of China.

REFERENCES

1. Tanabe, K., Misono, M., Ono, Y., and Hattori, H., "New Solid Acids and Bases." Kodansha, Tokyo, 1989.
2. Arata, K., *Adv. Catal.* **37**, 165 (1990).
3. Garin, F., Andriamasinoro, D., Abdulsamad, A., and Sommer, J., *J. Catal.* **131**, 199 (1991).
4. Davis, B. H., Keogh, R. A., and Srinivasan, R., *Catal. Today* **20**, 219 (1994).
5. Gao, Z., Chen, J. M., and Tang, Y., *Acta Chim. Sin.* **52**, 36 (1994).
6. Morterra, C., Cerrato, G., Pinna, F., Signoretto, M., and Strukul, G., *J. Catal.* **149**, 181 (1994).
7. Hsu, C. Y., Heimbuch, C. R., Armes, C. T., and Gates, B. C., *J. Chem. Soc. Chem. Commun.* 1645 (1992).
8. Jatia, A., Chang, C., MacLeod, J. D., Okubo, T., and Davis, M. E., *Catal. Lett.* **25**, 21 (1994).
9. Adeeva, V., de Haan, J. W., Janchen, J., Lei, G. D., Schunemann, V., van de Ven, L. J. M., Sachtler, W. M. H., and van Santen, R. A., *J. Catal.* **151**, 364 (1995).
10. Tabora, J. E., and Davis, R. J., *J. Chem. Soc. Faraday Trans.* **91**, 1825 (1995).
11. Coelho, M. A., Resasco, D. E., Sikabwe, E. C., and White, R. L., *Catal. Lett.* **32**, 253 (1995).
12. Miao, C. X., Hua, W. M., Chen, J. M., and Gao, Z., *Catal. Lett.* **37**, 187 (1996).
13. Miao, C. X., Hua, W. M., Chen, J. M., and Gao, Z., *Sci. China B* **39**, 406 (1996).
14. Song, X., and Sayari, A., *Catal. Rev.-Sci. Eng.* **38**, 329 (1996).
15. Miao, C. X., and Gao, Z., *Chem. J. Chin. Univ.* **18**, 424 (1997).
16. Gao, Z., Xia, Y. D., Hua, W. M., and Miao, C. X., *Top. Catal.* **6**, 101 (1998).
17. Olah, G. A., Malhotra, Narang, K. S. C., and Olah, J. A., *Synthesis* 672 (1978).
18. Arata, K., and Hino, M., *Bull. Chem. Soc. Jpn.* **53**, 446 (1980).
19. Arata, K., and Hino, M., *Appl. Catal.* **59**, 197 (1990).
20. Jia, C. G., Huang, M. Y., and Jiang, Y. Y., *Chin. J. Chem.* **11**, 452 (1993).
21. Xia, Y. D., Hua, W. M., and Gao, Z., *Catal. Lett.* **55**, 101 (1998).
22. Hino, M., and Arata, K., *J. Chem. Soc. Chem. Commun.* 851 (1980).
23. Ishida, T., Yamaguchi, T., and Tanabe, K., *Chem. Lett.* 1869 (1988).
24. Morterra, C., Cerrato, G., Pinna, F., and Signoretto, M., *J. Catal.* **151**, 109 (1995).
25. Stichert, W., and Schuth, F., *J. Catal.* **174**, 242 (1998).
26. Lee, J. S., and Park, D. S., *J. Catal.* **120**, 46 (1989).
27. Sikabwe, E. C., Coelho, M. A., Resasco, D. E., and White, R. L., *Catal. Lett.* **34**, 23 (1995).
28. Hua, W. M., Miao, C. X., Chen, J. M., and Gao, Z., *Mater. Chem. Phys.* **45**, 220 (1996).
29. Morterra, C., and Cerrato, G., *Phys. Chem. Chem. Phys.* **1**, 2825 (1999).
30. Hong, Z., Fogash, K. B., and Dumesic, J. A., *Catal. Today* **51**, 269 (1999).
31. Gao, Z., Chen, J. M., and Tang, Y., *Chem. J. Chin. Univ.* **14**, 658 (1993).
32. Jin, T., Yamaguchi, T., and Tanabe, K., *J. Phys. Chem.* **14**, 4794 (1986).
33. Gillespie, R. J., and Robinson, E. A., *Can. J. Chem.* **41**, 2074 (1963).
34. Spiewak, B. E., Handy, B. E., Sharma, S. B., and Dumesic, J. A., *Catal. Lett.* **23**, 207 (1994).
35. Damyanova, S., Grange, P., and Delmon, B., *J. Catal.* **168**, 421 (1997).
36. Djuricic, B., Pickering, S., Glaude, P., McGarry, D., and Tambuyser, P., *J. Mater. Sci.* **32**, 589 (1997).
37. Gao, Z., Chen, J. M., Hua, W. M., and Tang, Y., *Stud. Surf. Sci. Catal.* **90**, 507 (1994).
38. Arata, K., Yabe, K., and Toyoshima, I., *J. Catal.* **44**, 385 (1976).
39. Hino, M., and Arata, K., *Chem. Lett.* 325 (1978).
40. Guisnet, M. R., *Stud. Surf. Sci. Catal.* **20**, 283 (1985).
41. Guisnet, M. R., *Acc. Chem. Res.* **23**, 392 (1990).
42. Cardona-Martinez, N., and Dumesic, J. A., *Adv. Catal.* **38**, 149 (1992).
43. Sanderson, R. T., "Chemical Bonds and Bond Energy." Academic Press, New York, 1976.